Journal of Applied Analysis and Computation
Volume 14, Number 1, February 2024, 197–213
Website:http://www.jaac-online.com
DOI:10.11948/20230137

DYNAMICAL ANALYSIS OF SOLITONIC, QUASI-PERIODIC, BIFURCATION AND CHAOTIC PATTERNS OF LANDAU-GINZBURG-HIGGS MODEL

Nauman Raza[1,†], Syeda Sarwat Kazmi[1] and Ghada Ali Basendwah[2]

Abstract In this manuscript, the Landau-Ginzburg-Higgs (LGH) equation is considered as an investigating model. To extract novel results from the governing equation, the $G'/(bG'+G+a)$-expansion approach has been employed. Utilizing this approach, the outcomes are attained as hyperbolic and trigonometric functions. Kink, periodic and singular soliton solutions have been recovered by selecting the appropriate values for the parameters. The obtained findings for the LGH equation are displayed in 3-D, contour and 2-D profiles. Using Galilean transformation, the model is converted into a planar dynamical system, and qualitative analysis is investigated. Moreover, chaotic and quasi-periodic patterns have been addressed after including the perturbed term. Simulated results reveal that by modifying amplitude and frequency parameters, the dynamic behavior of the system can also be changed. The recorded results are novel and show the effectiveness and feasibility of the suggested technique for assessing soliton solutions and phase visualizations for different nonlinear models.

Keywords Landau-Ginzburg-Higgs equation, soliton solutions, the $G'/(bG'+G+a)$-expansion technique, bifurcation analysis, chaotic behavior.

MSC(2010) 78A60, 35Q51, 35Q55.

1. Introduction

In many scientific domains, nonlinear partial differential equations (NLPDEs) are beneficial in simulating complicated events that describe our day-to-day challenges. The use of nonlinear models has become increasingly pervasive in the fields of mathematics and engineering. The NLPDE covers an extensive variety of phenomena in nonlinear optics [39], plasma physics [1], population ecology [14], electromagnetic interactivity in plasma [38], and quantum theory [8]. Finding trustworthy analytical solutions for the NLPDE is a crucial research area since exact solutions capture the physical characteristics of nonlinear systems. A variety of potent techniques

[†]The corresponding author.
[1]Department of Mathematics, University of the Punjab, Quaid-e-Azam Campus, 54590 Lahore, Pakistan
[2]Department of Mathematics, King Abdulaziz University, Jeddah, Saudi Arabia
Email: nauman.math@pu.edu.pk(N. Raza), sarwatk323@gmail.com(S. S. Kazmi), gbasendwah@kau.edu.sa(G. A. Basendwah)

have been implemented to retrieve analytical solutions for NLPDEs; a few of them are the homotopy perturbation technique [17], Sardar sub-equation approach [29], residual power series technique [32], q-homotopy analysis approach [7], and Adomian decomposition approach [3].

The construction of soliton wave solutions for a broad range of NLPDEs has been exciting and inconceivable over the past few years. John Scott Russell's inspection of the translational wave marks the beginning of the history of solitons. Before Russell's theory was ultimately validated in the 1870s, eminent researchers and philosophers lauded its implications for science. In his 1872 research, Boussinesq widely used and anticipated key ideas that are still used today by futuristic scientists and thinkers. On the water wave equation, Boussinesq presented his perspective. His analysis reveals that the movement may be duplex as a result. Yet, the work of Boussinesq and Rayleigh continues to demonstrate the crucial problems of non-linearity and dispersion. Boussinesq's contribution was significant as it established the groundwork for constructing soliton wave solutions applicable to a wide range of NLPDEs. Optical solitons [15] are the basic molecules that keep the communications sector afloat. These underlying molecules provide the rules for how the internet industry, social networking sites, and other areas operate [16], [24].

Several strategies, including power series approach [34], F-expansion method [37], Hirota bilinear approach [2], Kudryashov approach [36] and many others [4,13, 26–28,35] have been designed to guarantee precise analytical solutions for NLPDEs in order to locate soliton solutions.

Investigating the LGH model is our primary goal in order to find soliton solutions. The Landau-Ginzburg-Higgs model has applications in several scientific and technical disciplines, including fiber optics, fluid mechanics, and chemical kinetics, among others. The LGH model has been examined using a few different techniques in the literature. Islam and Akbar [21] derived stable wave solutions to the LGH equation employing the improved Bernoulli sub-equation function technique (IBSEF); Iftikhar et al. [20] analyzed the LGH equation to extract traveling wave solutions; Ahmad et al. [5] obtained new precise results of the LGH equation utilizing the power index approach; Ali et al. [9] obtained traveling wave solutions for the LGH model employing inverse scattering transformation method; and Asjad et al. [12] analyzed the LGH model by using the generalized projective Riccati method to obtain soliton solutions.

To our knowledge, the LGH equation has not been scrutinized employing the $G'/(bG' + G + a)$-expansion approach [18] in previous literature. The purpose of this article is to employ the $G'/(bG' + G + a)$-expansion technique to extract analytical solutions for the LGH model. The current methodology offers certain benefits over earlier examined methodologies, as solutions are produced in a more general and explicit form, such as trigonometric functions and hyperbolic functions. The findings are graphically depicted in 3-D, contour, and 2-D plots for particular values of the involved parameters.

Employing chaos and bifurcation analysis to investigate differential equations (DEs) has been a renowned research field in recent years. These domains are regarded as useful tools for comprehending any physical process that is regulated by a DE. These nonlinear phenomena have been addressed in the field of engineering, ecology, telecommunications, and many others [22, 25, 30]. Time series, phase diagrams, and Poincaré maps are frequently employed methods when investigating dynamics of disturbed system and its chaotic nature [6].

• **Phase Plots:** Phase plots offer a graphical depiction of how a dynamic system behaves. They entail graphing one state variable against another. Analyzing the structure of the resulting graph can provide us with valuable information about the dynamics of the system, including its regularity, periodicity, or tendency towards chaos.

• **Time Series** A time series is a collection of data points gathered sequentially over a period of time. In this technique, the systemÂ's state variables are examined, and if they display random or unpredictable patterns, it is labeled as chaotic. On the other hand, if the variables demonstrate fixed point, periodic, or quasi-periodic behavior, they are considered non chaotic.

• **Poincaré Maps** Poincaré maps represent a specialized form of phase plot, concentrating on the points where the system trajectory intersects a specific surface or plane. Instead of plotting the whole trajectory, we concentrate solely on the instances it crosses the surface. This map furnishes essential insights into the system's characteristics, such as periodic patterns, stable regions, and the presence of bifurcations.

To our knowledge, the chaotic and qualitative analysis of the LGH model has not been examined in prior studies. Recently, Kazmi et al. [23] investigated the q-deformed Sinh-Gordon model by using bifurcation and chaos theory and obtained traveling wave solutions. Salman et al. [31] analyzed the bifurcation of the nonlinear Schrodinger equation and extracted soliton solutions. Alotaibi et al. [11] used bifurcation and chaotic patterns of the Fokas system to retrieve solitary wave solutions. Some captivating and recent work in this domain can be viewed in [33] and [10]. For bifurcation and chaotic behavior, phase portraits have been displayed with the aid of the mathematical application MATLAB.

The layout of the article is as follows: The Investigative Model is discussed in Section 2. Section 3 provides a complete overview of the suggested technique. Analytical solutions of the model under study are presented in Section 4, along with graphical representations. Section 5 is reserved for results and discussion. Qualitative analysis of the model is analyzed in section 6. The quasi-periodic and chaotic pattern are addressed in Section 7, and Section 8 deals with concluding remarks.

2. Investigating model

The Landau-Ginzburg-Higgs equation [19] is written as:

$$\frac{\partial^2 V}{\partial x^2} - \frac{\partial^2 V}{\partial t^2} - d^2 V + e^2 V^3 = 0, \tag{2.1}$$

where $V(x,t)$ represents ion-cyclotron wave for electrostatic potential, x and t denote the spatial and temporal coordinates, d and e are non-zero real constants.

By assuming the transformation as;

$$V(x,t) = V(\eta), \quad \eta = \lambda x - \mu t. \tag{2.2}$$

Here in Eq. (2.2), λ represents wave number and μ is the velocity of the traveling wave.

By plugging Eq. (2.2) into Eq. (2.1), we get the following ordinary differential equation;

$$\left(\mu^2 - \lambda^2\right) V''(\eta) - d^2 V(\eta) + e^2 V^3(\eta) = 0, \tag{2.3}$$

where $'$ denote the differentiation w.r.t η.

3. Premise of the suggested technique

With the aid of $G'/(bG'+G+a)$-expansion method, we will extract the precise solutions of the model under examination. By using this methodology, we can extract the findings in the form of trigonometric and hyperbolic functions.

Step 1. By taking non-linear partial differential equation (NLPDE) in the following manner;

$$F(x,t,\Re,\Re_x,\Re_t,\Re_{xx},\Re_{tt},...\Re_{xp})=0, \quad p\geq 0. \tag{3.1}$$

Here F is the polynomial including the unknown function $\Re(x,t)$. Then, by using the transformation given in Eq. (2.2), Eq. (3.1) is converted to ordinary differential equation as shown:

$$J(V,V',V'',...)=0, \tag{3.2}$$

here $'$ denoting the differentiation w.r.t η.

Step 2. Assume the solution of Eq. (3.2) is of the following form;

$$V(\eta)=\sum_{i=0}^{M} S_i Q^i(\eta), \tag{3.3}$$

where $Q=Q(\eta)=\frac{G'}{bG'+G+a}$, a and b are nonzero constants. $S_i's$ are arbitrary parameters to be evaluated later, $G=G(\eta)$ is the solution of following ODE:

$$G''=-\frac{\varrho}{b}G'-\frac{\vartheta}{b^2}G-\frac{\vartheta}{b^2}a,$$

here ϱ and ϑ are real numbers. Moreover, $Q=Q(\eta)$ satisfying the following ODE:

$$Q'=\frac{dQ(\eta)}{d\eta}=(\varrho-\vartheta-1)Q^2+\frac{(2\vartheta-\varrho)}{b}Q-\frac{\vartheta}{b^2}. \tag{3.4}$$

Step 3. The positive integer M can be evaluated by utilizing homogeneous balance principle between highest order derivative and non-linear term in Eq. (3.2).

Step 4. Equation.(3.4) possesses following types of solutions,

• **Type 1.** If $\kappa=\varrho^2-4\vartheta>0$, then $G=-a+n_1e^{\frac{1}{2b}(-\varrho-\sqrt{\kappa})\eta}+n_2e^{\frac{1}{2b}(-\varrho+\sqrt{\kappa})\eta}$, n_1 and n_2 are arbitrary constants satisfying $a^2+n_1^2+n_2^2\neq 0$.

In this type, $Q=Q(\eta)$ has the following representation:

$$Q_1=\frac{n_1(\varrho+\sqrt{\kappa})+n_2(\varrho-\sqrt{\kappa})e^{\frac{\sqrt{\kappa}}{b}\eta}}{b\ n_1(\varrho-2+\sqrt{\kappa})+b\ n_2(\varrho-2-\sqrt{\kappa})e^{\frac{\sqrt{\kappa}}{b}\eta}}.$$

We can also write $Q=Q(\eta)$ as;

$$Q_1=\frac{C_1\sinh(\frac{\sqrt{\kappa}}{2b}\eta)+C_2\cosh(\frac{\sqrt{\kappa}}{2b}\eta)}{C_3\sinh(\frac{\sqrt{\kappa}}{2b}\eta)+C_4\cosh(\frac{\sqrt{\kappa}}{2b}\eta)}.$$

Here
$C_1 = \varrho(n_2 - n_1) - \sqrt{\kappa}(n_2 + n_1)$,
$C_2 = \varrho(n_2 + n_1) - \sqrt{\kappa}(n_2 - n_1)$,
$C_3 = b\left((\varrho - 2)(n_2 - n_1) - \sqrt{\kappa}(n_2 + n_1)\right)$,
$C_4 = b\left((\varrho - 2)(n_2 + n_1) - \sqrt{\kappa}(n_2 - n_1)\right)$,

$$Q_1 = \begin{cases} Q_{1,1} = \frac{\varrho-2\vartheta}{2b(\varrho-\vartheta-1)} - \frac{\sqrt{\kappa}}{2b(\varrho-\vartheta-1)}\tanh(\frac{\sqrt{\kappa}}{2b}\eta), \\ \qquad\quad \text{if } (\varrho-2)(n_2-n_1) - \sqrt{\kappa}(n_2+n_1) = 0, \\ Q_{1,2} = \frac{\varrho-2\vartheta}{2b(\varrho-\vartheta-1)} - \frac{\sqrt{\kappa}}{2b(\varrho-\vartheta-1)}\coth(\frac{\sqrt{\kappa}}{2b}\eta), \\ \qquad\quad \text{if } (\varrho-2)(n_2+n_1) - \sqrt{\kappa}(n_2-n_1) = 0. \end{cases}$$

• **Type 2.** If $\kappa = \varrho^2 - 4\vartheta < 0$, then $G = -a + e^{\frac{-\varrho}{2b}\eta}\left(n_1\cos(\frac{\sqrt{-\kappa}}{2b}\eta) + n_2\sin(\frac{\sqrt{-\kappa}}{2b}\eta)\right)$.
In this type, $Q = Q(\eta)$ has the following representation:

$$Q_2 = \frac{\left(\varrho n_1 - \sqrt{-\kappa}n_2\right)\cos(\frac{\sqrt{-\kappa}}{2b}\eta) + \left(\varrho n_2 + \sqrt{-\kappa}n_1\right)\sin(\frac{\sqrt{-\kappa}}{2b}\eta)}{b\left((\varrho-2)n_1 - \sqrt{-\kappa}n_2\right)\cos(\frac{\sqrt{-\kappa}}{2b}\eta) + b\left((\varrho-2)n_2 + \sqrt{-\kappa}n_1\right)\sin(\frac{\sqrt{-\kappa}}{2b}\eta)},$$

$$Q_2 = \begin{cases} Q_{2,1} = \frac{\varrho-2\vartheta}{2b(\varrho-\vartheta-1)} + \frac{\sqrt{-\kappa}}{2b(\varrho-\vartheta-1)}\tan(\frac{\sqrt{-\kappa}}{2b}\eta), & \text{if } (\varrho-2)n_2 + \sqrt{-\kappa}n_1 = 0, \\ Q_{2,2} = \frac{\varrho-2\vartheta}{2b(\varrho-\vartheta-1)} - \frac{\sqrt{-\kappa}}{2b(\varrho-\vartheta-1)}\cot(\frac{\sqrt{-\kappa}}{2b}\eta), & \text{if } (\varrho-2)n_1 - \sqrt{-\kappa}n_2 = 0. \end{cases}$$

Step 5. By plugging Eq. (3.3) and Eq. (3.4) into Eq. (3.2) and reducing the coefficients of Q^i to zero yields a system of equations for $S_i's$. By solve the system of equations utilizing mathematical tool like Maple and plugging values of Q^i along with Eq. (3.3) and Eq. (2.2) into Eq. (2.1), we get solutions to Eq. (2.1).

The following section will provide the analytical solutions to the suggested model by employing $G'/(bG' + G + a)$-expansion approach.

4. Analytical solutions for the LGH model

In this portion, we will extract exact solutions of the proposed model by employing $G'/(bG' + G + a)$-expansion approach. By balancing the terms V^3 and V'' in Eq. (2.3) results $M = 1$.

4.1. The $G'/(bG' + G + a)$-expansion method

The $G'/(bG' + G + a)$-expansion approach is used for suggested model to get soliton solutions. According to given technique for $M = 1$, we make following assumption about initial solution:

$$V(\eta) = S_0 + S_1 Q(\eta), \tag{4.1}$$

where S_0 and S_1 are constants to be evaluated later. By plugging Eq. (3.4) and Eq. (4.1) into Eq. (2.3) and reducing the coefficients of Q^i to zero yields:

$$\begin{cases} Q^0 : e^2{S_0}^3 - d^2 S_0 = 0, \\ Q^1 : 2\left(-\lambda^2 + \mu^2\right)S_1\left(\varrho - \vartheta - 1\right)\left(2\vartheta - \varrho - \frac{\vartheta}{b^2}\right) - d^2 S_1 + 3e^2{S_0}^2 S_1 = 0, \\ Q^2 : 3e^2 S_0{S_1}^2 = 0, \\ Q^3 : 2\left(-\lambda^2 + \mu^2\right)S_1\left(\varrho - \vartheta - 1\right)^2 + e^2{S_1}^3 = 0. \end{cases}$$

With aid of mathematical tools, the following solutions can be determined.

$$S_0 = 0, \quad S_1 = \frac{bd}{e}\sqrt{-\frac{-\varrho+\vartheta+1}{\varrho b^2 - 2\,\vartheta b^2 + \vartheta}},$$
$$\mu = \sqrt{-\frac{-2\,b^2\lambda^2(\varrho^2+6\,\varrho\vartheta-4\,\vartheta^2+2\,\varrho-4\,\vartheta)-\vartheta\lambda^2(2\,\varrho+2\,\vartheta+2)-b^2d^2}{2\,b^2\varrho^2-6\,b^2\varrho\vartheta+4\,b^2\vartheta^2-2\,\varrho b^2+4\,\vartheta b^2+2\,\varrho\vartheta-2\,\vartheta^2-2\,\vartheta}}.$$

- **Type 1.** For $\kappa = \varrho^2 - 4\vartheta > 0$, we have following solutions,

$$V_1(x,t) = \frac{bd}{e}\sqrt{-\frac{-\varrho+\vartheta+1}{\varrho b^2 - 2\,\vartheta b^2 + \vartheta}}Q_1, \tag{4.2}$$

where

$$Q_1 = \frac{C_1\sinh(\frac{\sqrt{\kappa}}{2b}\eta) + C_2\cosh(\frac{\sqrt{\kappa}}{2b}\eta)}{C_3\sinh(\frac{\sqrt{\kappa}}{2b}\eta) + C_4\cosh(\frac{\sqrt{\kappa}}{2b}\eta)}.$$

Here
$C_1 = \varrho(n_2 - n_1) - \sqrt{\kappa}(n_2 + n_1)$,
$C_2 = \varrho(n_2 + n_1) - \sqrt{\kappa}(n_2 - n_1)$,
$C_3 = b\,((\varrho - 2)(n_2 - n_1) - \sqrt{\kappa}(n_2 + n_1))$,
$C_4 = b\,((\varrho - 2)(n_2 + n_1) - \sqrt{\kappa}(n_2 - n_1))$.

If $(\varrho - 2)(n_2 - n_1) - \sqrt{\kappa}(n_2 + n_1) = 0$, then Eq. (4.2) becomes

$$V_{1,1}(x,t) = \frac{bd}{e}\sqrt{-\frac{-\varrho+\vartheta+1}{\varrho b^2 - 2\,\vartheta b^2 + \vartheta}}Q_{1,1}, \tag{4.3}$$

here

$$Q_{1,1} = \frac{\varrho - 2\vartheta}{2b(\varrho - \vartheta - 1)} - \frac{\sqrt{\kappa}}{2b(\varrho - \vartheta - 1)}\tanh(\frac{\sqrt{\kappa}}{2b}\eta).$$

Moreover, if $(\varrho - 2)(n_2 + n_1) - \sqrt{\kappa}(n_2 - n_1) = 0$, then Eq. (4.2) becomes

$$V_{1,2}(x,t) = \frac{bd}{e}\sqrt{-\frac{-\varrho+\vartheta+1}{\varrho b^2 - 2\,\vartheta b^2 + \varrho}}Q_{1,2}, \tag{4.4}$$

where

$$Q_{1,2} = \frac{\varrho - 2\varrho}{2b(\varrho - \vartheta - 1)} - \frac{\sqrt{\kappa}}{2b(\varrho - \vartheta - 1)}\coth(\frac{\sqrt{\kappa}}{2b}\eta),$$

with $\eta = \lambda x - \mu t$.

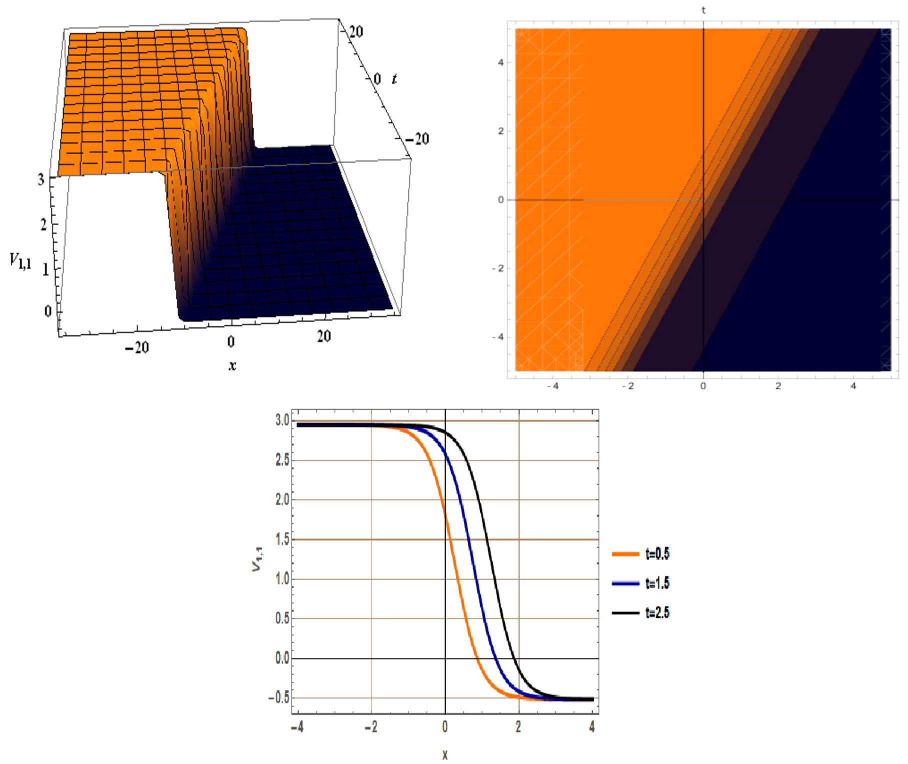

Figure 1. 3D, Contour and 2D plot for $V_{1,1}(x,t)$ by taking $\varrho = 2$, $\lambda = 2$, $\vartheta = 0.5$, $b = 1$, $d = 2.1$, $e = 1$ and $\mu = 1$.

• **Type 2.** For $\kappa = \varrho^2 - 4\vartheta < 0$, we have

$$V_2(x,t) = \frac{bd}{e}\sqrt{-\frac{-\varrho+\vartheta+1}{\varrho b^2 - 2\,\vartheta b^2 + \vartheta}Q_2}, \tag{4.5}$$

where

$$Q_2 = \frac{\left(\varrho n_1 - \sqrt{-\kappa}n_2\right)\cos(\frac{\sqrt{-\kappa}}{2b}\eta) + \left(\varrho n_2 - \sqrt{-\kappa}n_1\right)\sin(\frac{\sqrt{-\kappa}}{2b}\eta)}{b\left((\varrho-2)n_1 - \sqrt{-\kappa}n_2\right)\cos(\frac{\sqrt{-\kappa}}{2b}\eta) + b\left((\varrho-2)n_2 + \sqrt{-\kappa}n_1\right)\sin(\frac{\sqrt{-\kappa}}{2b}\eta)}.$$

If $(\varrho-2)n_2 + \sqrt{-\kappa}n_1 = 0$, then Eq. (4.5) becomes

$$V_{2,1}(x,t) = \frac{bd}{e}\sqrt{-\frac{-\varrho+\vartheta+1}{\varrho b^2 - 2\,\vartheta b^2 + \vartheta}Q_{2,1}}, \tag{4.6}$$

here

$$Q_{2,1} = \frac{\varrho - 2\vartheta}{2b(\varrho-\vartheta-1)} + \frac{\sqrt{-\kappa}}{2b(\varrho-\vartheta-1)}\tan(\frac{\sqrt{-\kappa}}{2b}\eta)).$$

Further, if $(\varrho-2)n_1 - \sqrt{-\kappa}n_2 = 0$, then Eq. (4.5) becomes

$$V_{2,2}(x,t) = \frac{bd}{e}\sqrt{-\frac{-\varrho+\vartheta+1}{\varrho b^2 - 2\,\vartheta b^2 + \vartheta}Q_{2,2}}, \tag{4.7}$$

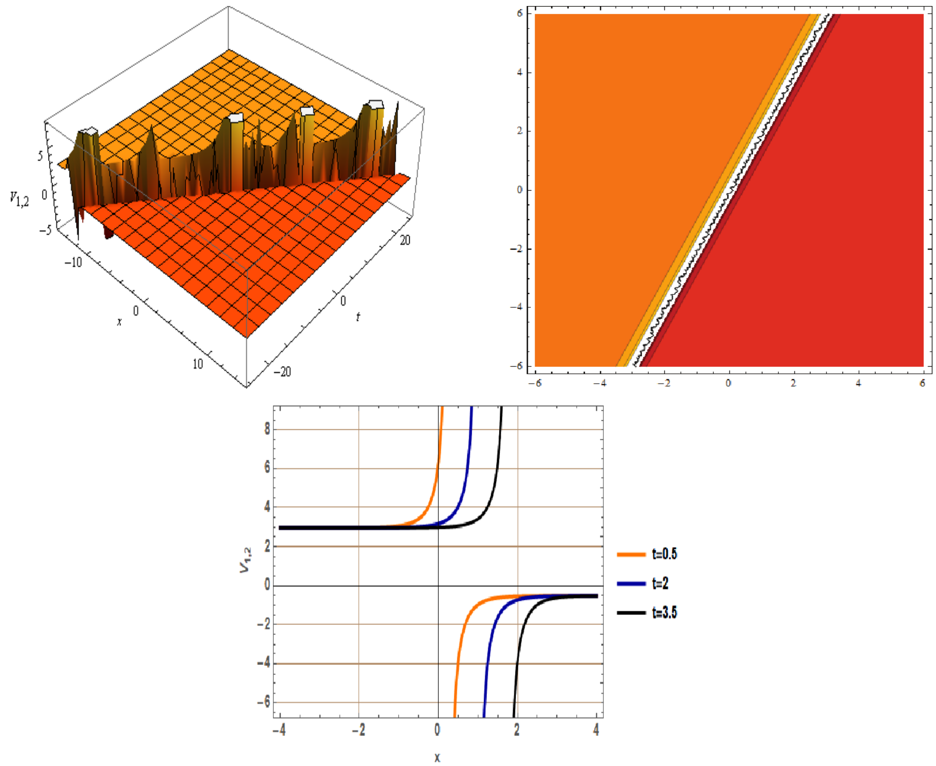

Figure 2. 3D, Contour and 2D plot for $V_{1,2}(x, t)$ by taking $\varrho = 2$, $\lambda = 2$, $\vartheta = 0.5$, $b = 1$, $d = 2.1$, $e = 1$ and $\mu = 1$.

where

$$Q_{2,2} = \frac{\varrho - 2\vartheta}{2b(\varrho - \vartheta - 1)} - \frac{\sqrt{-\kappa}}{2b(\varrho - \vartheta - 1)} \cot(\frac{\sqrt{-\kappa}}{2b}\eta),$$

with $\eta = \lambda x - \mu t$.

5. Results and discussion

In this portion, the obtained results for the LGH model have been illustrated graphically. By accepting various specific values ofÂ the parameters for each outcome, we created a variety of soliton profiles by employing $G'/(bG' + G + a)$-expansion approach. The recorded results are displayed as 3D, contour and 2D graphical patterns. It is worth noting that the findings presented in this paper have been compared with [12]. The comparison revealed that the extracted outcomes are novel and have not been previously documented.

• In Fig.(1) **kink solitons** of $V_{1,1}$ have been detected for $\varrho = 2$, $\lambda = 2$, $\vartheta = 0.5$, $b = 1$, $d = 2.1$, $e = 1$ and $\mu = 1$.
• Fig.(2) illustrates **singular soliton patterns** for $V_{1,2}$ by selecting appropriate parameters.
• The graphical visualization for $V_{2,1}$ has been addressed in Fig.(3) by selecting

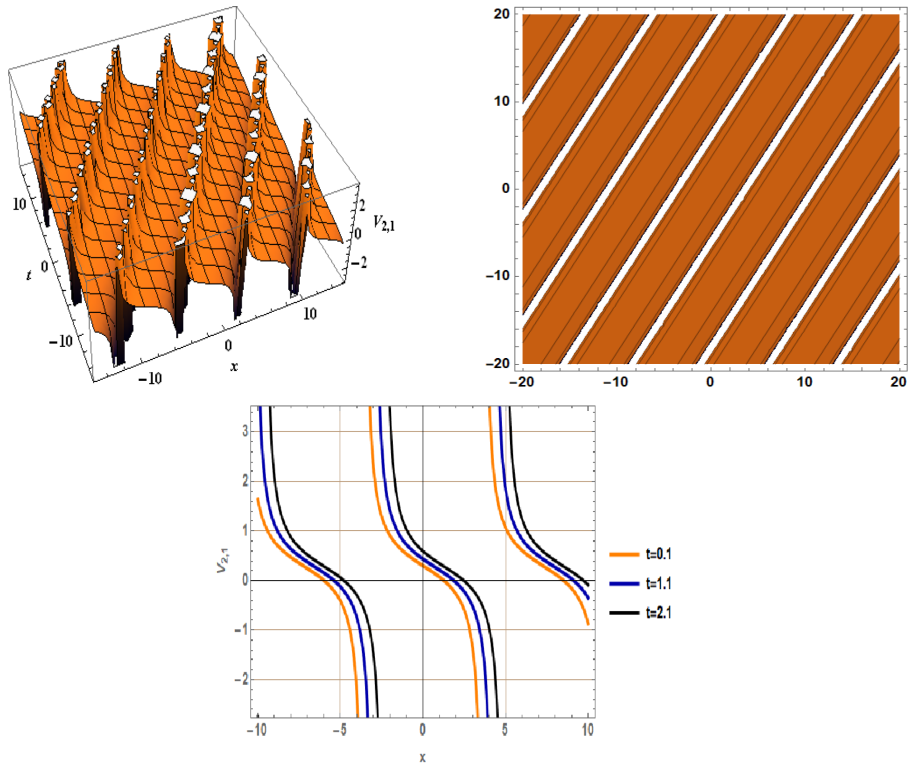

Figure 3. 3D, Contour and 2D plot for $V_{2,1}(x,t)$ by taking $\varrho = 1$, $\lambda = 1$, $\vartheta = 1$, $b = 2$, $d = 1$, $e = 1$ and $\mu = 0.6$.

$\varrho = 1$, $\lambda = 1$, $\vartheta = 1$, $b = 2$, $d = 1$, $e = 1$ and $\mu = 0.6$.
• In Fig.(4), **singular solitons** have been retrieved for $V_{2,2}$ by adjusting particular values for parameters: $\varrho = 1$, $\lambda = 1$, $\vartheta = 1$, $b = 2$, $d = 1$, $e = 1$ and $\mu = 0.6$.

6. Bifurcation analysis of the LGH model

In this section, we shall analyze Eq. (2.1) using qualitative analysis. Applying the Galilean transformation, Eq. (2.3) may be expressed as a planar dynamical system.

$$\begin{cases} \frac{dV}{d\eta} = U, \\ \frac{dU}{d\eta} = \zeta_1 V - \zeta_2 V^3, \end{cases} \tag{6.1}$$

where $\zeta_1 = \frac{d^2}{\mu^2-\lambda^2}$ and $\zeta_2 = \frac{e^2}{\mu^2-\lambda^2}$. The above system of ODEs is Hamiltonian, and has the integral as follows;

$$R(V,U) = \frac{U^2}{2} - \zeta_1 \frac{V^2}{2} + \zeta_2 \frac{V^4}{4} = r, \tag{6.2}$$

where r is the Hamiltonian parameter. Now, we will investigate bifurcation and phase visualization for system (6.1). The outcomes of our qualitative analysis are as follows. Firstly, observe that system (6.1) possesses three equilibrium points as

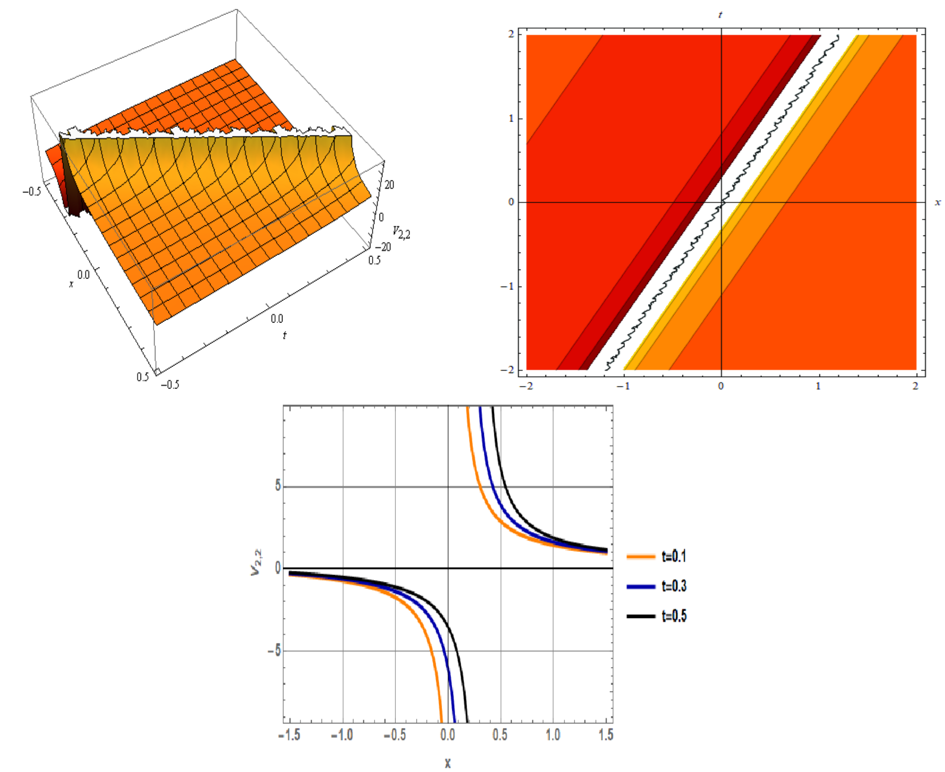

Figure 4. 3D, Contour and 2D plot for $V_{2,2}(x,t)$ by taking $\varrho = 1$, $\lambda = 1$, $\vartheta = 1$, $b = 2$, $d = 1$, $e = 1$ and $\mu = 0.6$.

follows:

$$N_1 = (0,0), \quad N_2 = (\sqrt{\frac{\zeta_1}{\zeta_2}}, 0), \quad N_3 = (-\sqrt{\frac{\zeta_1}{\zeta_2}}, 0).$$

Moreover, the system's Jacobian will be:

$$J(V,U) = \begin{pmatrix} 0 & 1 \\ \zeta_1 - 3\zeta_2 V^2 & 0 \end{pmatrix}. \tag{6.3}$$

Let $\mathcal{F}$ and $\mathcal{C}$ represent the determinant and trace of the Jacobian matrix (6.3) at the fixed point N_i, and they are given as:

$$\mathcal{C} = trace(J)|_{N_i} = 0, \quad \mathcal{F} = det(J)|_{N_i} = -\zeta_1 + 3\zeta_2 V^2.$$

For phase plots at equilibrium points, it is known that a point is saddle if $\mathcal{F} < 0$, a cusp if $\mathcal{F} > 0$, and a center if $\mathcal{F} = 0$. The following results are possible by giving the parameters varying values.

• **Case 5.1.** Let $\zeta_1 > 0$ and $\zeta_2 > 0$
For $d = 4$, $e = 4$, $\mu = 5$ and $\lambda = 3$, system (6.1) possess three points $N_1 = (0,0)$,

$N_2 = (1, 0)$, $N_3 = (-1, 0)$ as equilibrium points. Considering such case N_1 is **saddle point** and N_2, N_3 depict a **center**. These points are displayed in Fig.(5).

• **Case 5.2.** Let $\zeta_1 < 0$ and $\zeta_2 < 0$
For $d = 4$, $e = 4$, $\mu = 3$ and $\lambda = 5$, system (6.1) possess three points $N_1 = (0, 0)$, $N_2 = (1, 0)$, $N_3 = (-1, 0)$ as equilibrium points. Considering such case N_1 is **central point** and N_2, N_3 are **saddle points**. These points are presented in Fig.(6).

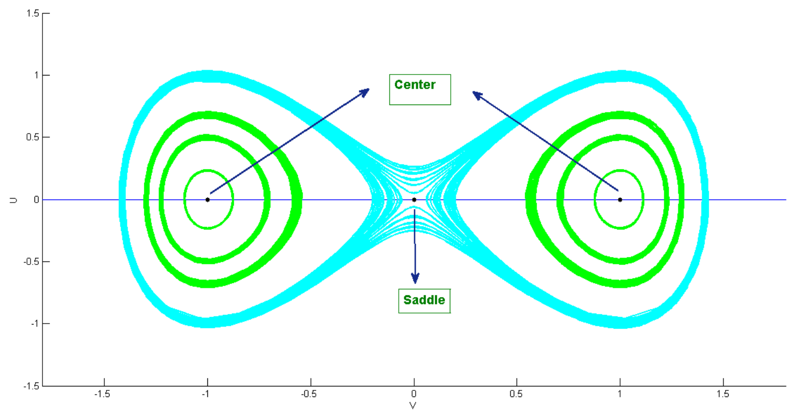

Figure 5. Phase portrait for system (6.1), when $\zeta_1 > 0$ and $\zeta_2 > 0$.

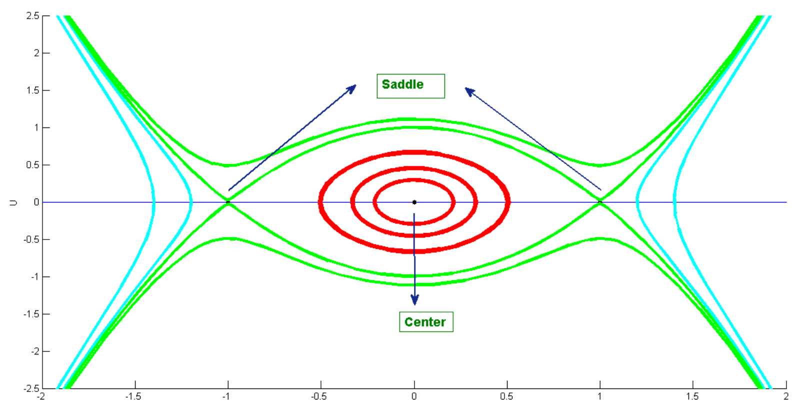

Figure 6. Phase portrait for system (6.1), when $\zeta_1 < 0$ and $\zeta_2 < 0$.

7. Chaotic and quasi periodic behaviors

In this portion, we will analyze the quasi periodic and chaotic patterns of Eq. (2.1). To investigate these patterns, we will add a periodic term $\delta_0 \cos(\omega\eta)$ to the dynamical system (6.1), where δ_0 is the amplitude and ω is the frequency of the perturbed term. In this way, the dynamical system (6.1) with perturbed term is as follows:

$$\begin{cases} \frac{dV}{d\eta} = U, \\ \frac{dU}{d\eta} = \zeta_1 V - \zeta_2 V^3 + \delta_0 \cos(\omega\eta), \end{cases} \tag{7.1}$$

where $\zeta_1 = \frac{d^2}{\mu^2-\lambda^2}$ and $\zeta_2 = \frac{e^2}{\mu^2-\lambda^2}$.

Several random physical parameter values are tried in order to identify Â dynamical behaviors of the perturbed Â equation, Â and various result are recorded. We have explored the quasi-periodic and chaotic nature described of system (7.1) using a range of tools like phase plots, time plots, and Poincaré maps. To thoroughly investigate the issue, we will assess how the parameters ζ_1, ζ_2, δ_0, and ω affect it in two distinct scenarios. In the first case, we will hold all parameters constant except the amplitude δ_0, while in the second, we will investigate the consequences of changing both δ_0 and ω while keeping the other parameters unchanged.

- 3D, time analysis graph, 2D and Poincaré maps are displayed in Fig.(7) for $\zeta_1 = -3.2$, $\zeta_2 = 1.1$, $\delta_0 = 0.5$ and $\omega = \pi$. In this case both amplitude and frequency of external force are very small and it is observed that the perturbed system (7.1) exhibits periodic behavior.

- Fig.(8) presents the 3D, 2D, time analysis graph and Poincaré maps by increasing amplitude as $\delta_0 = 1.5$, and it is detected that the modified dynamical system (7.1) exhibits quasi-periodic behavior.

- In Fig.(9), 3D and 2D phase images, time analysis and Poincaré maps are presented for $\zeta_1 = -3.2$, $\zeta_2 = 1.1$, $\delta_0 = 4.5$ and $\omega = 2\pi$. It is revealed that by changing these parameters, the disturbed system (7.1) shows quasi-periodic chaotic pattern.

- In Fig.(10), the influence of varying amplitude and frequency is analyzed as in this case $\delta_0 = 5.5$ and $\omega = 3\pi$, and it is observed that the modified system (7.1) exhibits chaotic behavior. Additionally, the Poincaré map displays numerous scattered points, providing further confirmation of the chaotic nature of the system.

8. Conclusion

In this manuscript, the Landau-Ginzburg-Higgs (LGH) equation was considered as an investigating model. To extract novel results from the governing equation, the $G'/(bG' + G + a)$-expansion approach had been employed. Utilizing this approach, the outcomes were attained as hyperbolic and trigonometric functions. Kink, singular and periodic soliton solutions had been recovered by selecting the appropriate values for the parameters. The obtained findings for the LGH equation were displayed in 3-D, Contour and 2-D profiles. Using Galilean transformation, the model was converted into a planar dynamical system, and qualitative analysis was investigated. Bifurcation of the governing model has been analyzed for system (6.1) at the fixed points. Also the phase plots have been presented in Figs.(5)-(6). Moreover, an external periodic force has been added into dynamical system, and different tools, such as phase plots, Poincaré map, and time plots, has been utilized for investigating the quasi-periodic and chaotic nature of disturbed system (7.1). Simulated results reveal that by modifying amplitude and frequency parameters, the dynamic behavior of the system can also be changed. The recorded results were novel and

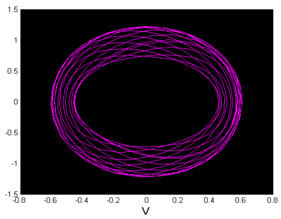

(a) 2D-Plot

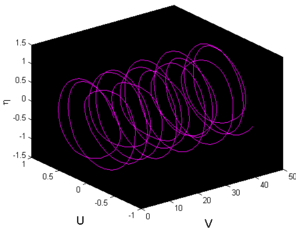

(b) 3D-Plot

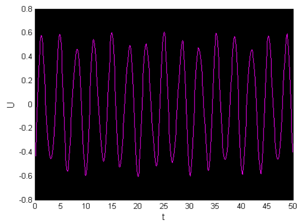

(c) Time Analysis

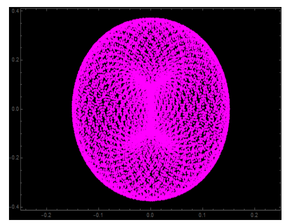

(d) Poincare map

Figure 7. For $\zeta_1 = -3.2$, $\zeta_2 = 1.1$, $\delta_0 = 0.5$ and $\omega = \pi$, the system (7.1) is displayed for initial condition (0.5,0.5).

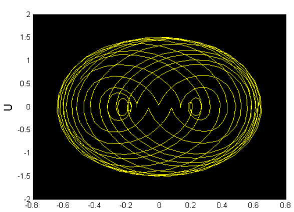

(a) 2D-Plot

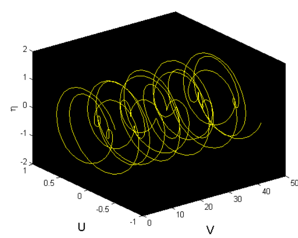

(b) 3D-Plot

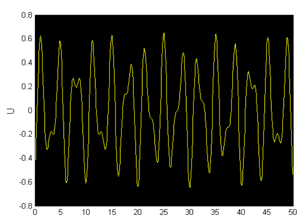

(c) Time Analysis

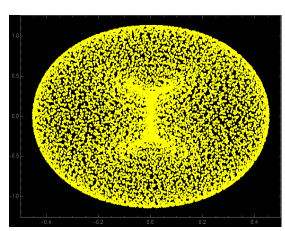

(d) Poincare map

Figure 8. For $\zeta_1 = -3.2$, $\zeta_2 = 1.1$, $\delta_0 = 1.5$ and $\omega = \pi$, the system (7.1) is displayed for initial condition (0.5,0.5).

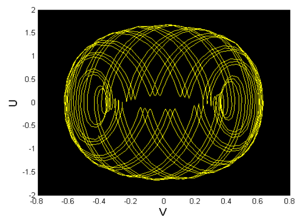

(a) 2D-Plot

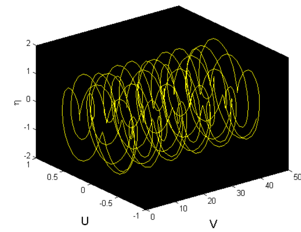

(b) 3D-Plot

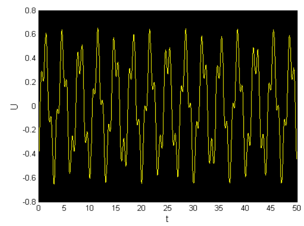

(c) Time Analysis

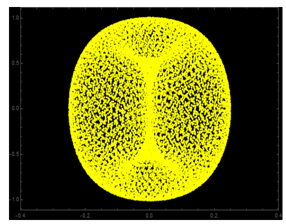

(d) Poincare map

Figure 9. For $\zeta_1 = -3.2$, $\zeta_2 = 1.1$, $\delta_0 = 4.5$ and $\omega = 2\pi$, the system (7.1) is displayed for initial condition (0.5,0.5).

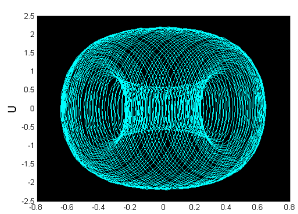

(a) 2D-Plot

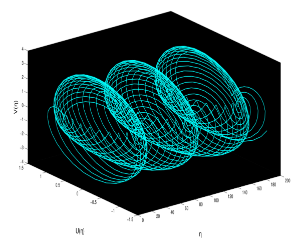

(b) 3D-Plot

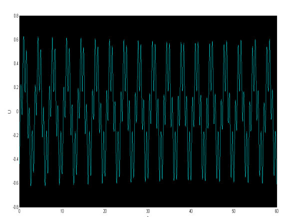

(c) Time Analysis

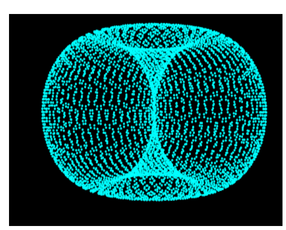

(d) Poincare map

Figure 10. For $\zeta_1 = -3.2$, $\zeta_2 = 1.1$, $\delta_0 = 5.5$ and $\omega = 3\pi$, the system (7.1) is displayed for initial condition (0.5,0.5).

show the effectiveness and feasibility of the suggested technique for assessing soliton solutions and phase visualizations for different nonlinear models.

References

[1] M. A. Abdou, *An analytical method for space-time fractional nonlinear differential equations arising in plasma physics*, Journal of Ocean Engineering and Science, 2017, 2(4), 288–292.

[2] T. Abdulkadir Sulaiman and A. Yusuf, *Dynamics of lump-periodic and breather waves solutions with variable coefficients in liquid with gas bubbles*, Waves in Random and Complex Media, 2021, 1–14.

[3] G. Adomian, *Solving frontier problems of physics: The decomposition method*, Springer Science and Business Media, 2013, 60.

[4] I. Ahmad, A. Jalil, A. Ullah, S. Ahmad and M. De la Sen, *Some new exact solutions of (4+ 1)-dimensional Davey—Stewartson-Kadomtsev—Petviashvili equation*, Results in Physics, 2023, 45, 106240.

[5] K. Ahmad, K. Bibi, M. S. Arif and K. Abodayeh, *New Exact Solutions of Landau-Ginzburg-Higgs Equation Using Power Index Method*, Journal of Function Spaces, 2023.

[6] Ö. Z. E. R. Ahmet and A. K. I. N. Erhan, *Tools for detecting chaos*, Sakarya University Journal of Science, 2005, 9(1), 60–66.

[7] L. Akinyemi, *q-Homotopy analysis method for solving the seventh-order time-fractional LaxÂ's KortewegÂ–de Vries and SawadaÂ–Kotera equations*, Computational and Applied Mathematics, 2019, 38(4), 191.

[8] L. Akinyemi, H. Rezazadeh, S. W. Yao, M. A. Akbar, M. M. Khater, A. Jhangeer, M. Inc and H. Ahmad, *Nonlinear dispersion in parabolic law medium and its optical solitons*, Results in Physics, 2021, 26, 104411.

[9] M. R. Ali, M. A. Khattab and S. M. Mabrouk, *Travelling wave solution for the Landau-Ginburg-Higgs model via the inverse scattering transformation method*, Nonlinear Dynamics, 2023, 1–11.

[10] H. Almusawa, A. Jhangeer and Z. Hussain, *Observation on different dynamics of breaking soliton equation by bifurcation analysis and multistability theory*, Results in Physics, 2022, 36, 105364.

[11] M. F. Alotaibi, N. Raza, M. H. Rafiq and A. Soltani, *New solitary waves, bifurcation and chaotic patterns of Fokas system arising in monomode fiber communication system*, Alexandria Engineering Journal, 2023, 67, 583–595.

[12] M. I. Asjad, S. Z. Majid, W. A. Faridi and S. M. Eldin, *Sensitive analysis of soliton solutions of nonlinear Landau-Ginzburg-Higgs equation with generalized projective Riccati method*, AIMS Mathematics, 2023, 8(5), 10210–10227.

[13] D. Baleanu, M. S. Osman, A. Zubair, N. Raza, O. A. Arqub and W. X. Ma, *Soliton solutions of a nonlinear fractional Sasa-Satsuma equation in monomode optical fibers*, Applied Mathematics and Information Sciences, 2020, 14(3), 365–374.

[14] O. A. Bruzzone, D. V. Perri and M. H. Easdale, *Vegetation responses to variations in climate: A combined ordinary differential equation and sequential Monte Carlo estimation approach*, Ecological Informatics, 2023, 73.

[15] C. Gu, *Soliton Theory and its Applications*, Springer Science and Business Media, 2013.

[16] A. Hasegawa, Y. Kodama and A. Maruta, *Recent progress in dispersion-managed soliton transmission technologies*, Optical Fiber Technology, 1997, 3(3), 197–213.

[17] J. H. He, *Homotopy perturbation technique*, Computer methods in applied mechanics and engineering, 1999, 178(3–4), 257–262.

[18] B. Hong, *Assorted exact explicit solutions for the generalized Atangana's fractional BBM-Burgers equation with the dissipative term*, Frontiers in Physics, 2022, 10, 1152.

[19] W. P. Hu, Z. C. Deng, S. M. Han and W. Fa, *Multi-symplectic Runge-Kutta methods for Landau-Ginzburg-Higgs equation*, Applied Mathematics and Mechanics, 2009, 30(8), 1027–1034.

[20] A. Iftikhar, A. Ghafoor, T. Zubair, S. Firdous and S. T. Mohyud-Din, *Solutions of (2+ 1) dimensional generalized KdV, Sin Gordon and Landau-Ginzburg-Higgs Equations*, Scientific Research and Essays, 2013, 8(28), 1349–1359.

[21] M. E. Islam and M. A. Akbar, *Stable wave solutions to the Landau-Ginzburg-Higgs equation and the modified equal width wave equation using the IBSEF method*, Arab Journal of Basic and Applied Sciences, 2020, 27(1), 270–278.

[22] A. Jhangeer, A. Hussain, M. Junaid-U-Rehman, D. Baleanu and M. B. Riaz, *Quasi-periodic, chaotic and travelling wave structures of modified Gardner equation*, Chaos, Solitons and Fractals, 2021, 143, 110578.

[23] S. S. Kazmi, A. Jhangeer, N. Raza, H. I. Alrebdi, A. H. Abdel-Aty and H. Eleuch, *The analysis of bifurcation, quasi-periodic and solitons patterns to the new form of the generalized q-deformed Sinh-Gordon equation*, Symmetry, 2023, 15(7), 1324.

[24] Y. S. Kivshar and G. Agrawal, *Optical Solitons: From Fibers to Photonic Crystals*, Academic Press., 2003.

[25] J. Li and F. Chen, *Bifurcations and exact traveling wave solutions of degenerate coupled multi-KdV equations*, International Journal of Bifurcation and Chaos, 2016, 26(03), 1650045.

[26] C. R. Qin and J. G. Liu, *Study on double-periodic soliton and non-traveling wave solutions of integrable systems with variable coefficients*, Results in Physics, 2022, 34, 105254.

[27] N. Raza, M. R. Aslam and H. Rezazadeh, *Analytical study of resonant optical solitons with variable coefficients in Kerr and non-Kerr law media*, Optical and Quantum Electronics, 2019, 51, 1–12.

[28] N. Raza and S. S. Kazmi, *Qualitative analysis and stationary optical patterns of nonlinear Schrödinger equation including nonlinear chromatic dispersion*, Optical and Quantum Electronics, 2023, 55(8), 718.

[29] H. Rezazadeh, M. Inc and D. Baleanu, *New solitary wave solutions for variants of (3+ 1)-dimensional Wazwaz-Benjamin-Bona-Mahony equations*, Frontiers in Physics, 2020, 8, 332.

[30] A. Saha, *Bifurcation, periodic and chaotic motions of the modified equal width-Burgers (MEW-Burgers) equation with external periodic perturbation*, Nonlinear Dynamics, 2017, 87(4), 2193–2201.

[31] F. Salman, N. Raza, G. A. Basendwah and M. M. Jaradat, *Optical solitons and qualitative analysis of nonlinear Schrodinger equation in the presence of self steepening and self frequency shift*, Results in Physics, 2022, 39, 105753.

[32] M. Senol, O. S. Iyiola, H. Daei Kasmaei and L. Akinyemi, *Efficient analytical techniques for solving time-fractional nonlinear coupled Jaulent–Miodek system with energy-dependent Schrödinger potential*, Advances in Difference Equations, 2019, 1–21.

[33] L. Tang, *Bifurcation analysis and multiple solitons in birefringent fibers with coupled Schrödinger-Hirota equation*, Chaos, Solitons and Fractals, 2022, 161, 112383.

[34] S. F. Tian, M. J. Xu and T. T. Zhang, *A symmetry-preserving difference scheme and analytical solutions of a generalized higher-order beam equation*, Proceedings of the Royal Society A, 2021, 477(2255), 20210455.

[35] A. M. Wazwaz, *Multiple-soliton solutions for a (3+ 1)-dimensional generalized KP equation*, Communications in Nonlinear Science and Numerical Simulation, 2012, 17(2), 491–495.

[36] A. Zafar, M. Shakeel, A. Ali, L. Akinyemi and H. Rezazadeh, *Optical solitons of nonlinear complex Ginzburg–Landau equation via two modified expansion schemes*, Optical and Quantum Electronics, 2022, 54, 1–15.

[37] E. M. Zayed, K. A. Gepreel, R. M. Shohib, M. E. Alngar and Y. Yildirim, *Optical solitons for the perturbed Biswas-Milovic equation with Kudryashov's law of refractive index by the unified auxiliary equation method*, Optik., 2021, 230, 166286.

[38] T. Y. Zhou, B. Tian, C. R. Zhang and S. H. Liu, *Auto-Bäcklund transformations, bilinear forms, multiple-soliton, quasi-soliton and hybrid solutions of a (3+ 1)-dimensional modified Korteweg-de Vries-Zakharov-Kuznetsov equation in an electron-positron plasma*, The European Physical Journal Plus, 2022, 137(8), 912.

[39] A. Zubair, N. Raza, M. Mirzazadeh, W. Liu and Q. Zhou, *Analytic study on optical solitons in parity-time-symmetric mixed linear and nonlinear modulation lattices with non-Kerr nonlinearities*, Optik., 2018, 173, 249–262.